AADE-18-FTCE-096

Parametric Analysis of Efficiency Using an Efficient Mud Displacement Modeling Technique

Yanfang Wang, Louisiana State University; Hu Dai, Pegasus Vertex, Inc.

Abstract

As advanced drilling methods such as directional horizontal drilling are growing in popularity in the development of unconventional reservoirs, an improved understanding and techniques of cement planning and design are demanding to achieve better zonal isolation. Displacement efficiency is used to evaluate the success of cementing jobs. Many critical factors affect the outcome of displacement, which are but not limited to flow patterns, well deviations, standoff, pipe movements and fluid rheological behaviors.

In order to model fluid flow and transport in the annulus, a cementing simulator was developed using finite volume method to solve the fluid flow and concentration transport. In order to highlight the robustness of the simulator, a model was created in a state-of-the-art CFD software to verify the simulator. The CFD model was validated by an experimental study for both concentric and eccentric cases with the effect of flow rates (Reynolds numbers) and density contrasts. A systematic study was conducted to identify practical guidelines for optimum cementing design. The effects of well deviation (vertical and horizontal wells), displacement flow rates and standoffs were taken into account. Non-Newtonian fluid rheology was also considered in the analysis.

The cementing simulator was able to simulate two or more phases (i.e. mud-spacer-cement) with the calculation of fluid concentration change at each depth and each azimuthal location and determines flow regime by calculating the critical Reynolds number. Comparison of simulation times between the cementing simulator and the CFD model for each case also demonstrated the effectiveness of this simulator.

Introduction

The modeling of mud displacement and cement placement has been investigated broadly, from analytically to experimentally, and to nowadays advanced CFD modeling. In order to optimize the cementing job, the calculation and evaluation of displacement efficiency is a crucial step before execution. There are many causes for cement displacement problems and inefficiencies, including poor borehole conditioning, inappropriate displacement flow rates, insufficient casing centralization, density and viscosity hierarchy leading to interface instabilities. In order to evaluate the bonding between casing and wellbore after a cementing job, cement bond logs provide the information including the bond, the fluid interface between mud and cement (including spacer), and axial velocity profiles in the post job analysis. However, when logging operations indicate that the cement job is defective, either in the form of poor cement bonding or communication between zones, a remedial cementing technique called Squeeze Cementing (Farkas et al., 1999) has to be performed to establish zonal isolation, which is much more expensive than the primary cementing job. Therefore, it should be emphasized that an accurate and reliable cementing job design technique is demanding throughout the whole cementing process.

Cementing process has many similarities with hole cleaning while drilling (Hemphill and Ravi, 2006). Usually, the sequence of fluid injection is to pump preflush such as water, at first to avoid the problems due to the direct contact between drilling mud and cement slurry. And then one kind of heavier fluid called spacer is often pumped also to separate drilling mud and cement, and also helps to remove drilling mud. Next is to pump lead cement, tail cement, and displacing fluid. Studies have shown that it is more efficient to displace a lighter and less viscous fluid by a denser and more viscous fluid. Thus, density hierarchy and viscosity hierarchy are really important in the cementing job design.

The importance of casing centralization has been understood and emphasized since the early days of cementing. Sometimes the term of standoff (SO) is used to describe how much the pipe is centered. If a casing is perfectly centered, the standoff is 100%, and a standoff of 0% means the pipe touches the wellbore. In this study, we use the term of eccentricity, which is also frequently used in the oilfield. An eccentricity of 0 stands for a perfectly centered pipe. Liu and Weber (2012) introduced a computer modeling technique to evaluate and optimize centralizer placement for cementing jobs. However, due to many reasons, a perfectly centralized pipe or casing is very hard to achieve. Siginer and Bakhtiyarov (1998) investigated the effect of pipe eccentricity on the fluid flow in annuli both analytically and numerically.

Pipe rotation becomes significant in non-ideal conditions such as high eccentricity. As known from hole cleaning, pipe rotation helps to remove cuttings efficiently from the narrow annulus (Hemphill and Ravi, 2005). In cementing, without pipe rotation, the fluid flows preferentially through the wider

annulus, which is more likely to cause mud channeling and leave mud behind the dominate flow. Moroni et al. (2009) presented the modeling technique to investigate the effect of pipe rotation on hole cleaning and cement-slurry placement. Their results were matched with field validation and show that pipe movement improved the cementing job and zonal isolation. Therefore, with sufficient pipe rotation speeds, the cementing job can be so efficient that saves potential remedial costs.

Displacement efficiency is defined as the volume fraction of displacing fluid in the annulus. This is equivalent to the volume of displaced fluid removed from the annulus divided by the annulus volume. At the beginning of displacing process, the volume of cement pumped is almost equal to the volume of mud displaced, which means the displacement efficiency is proportional to flow rate (Tehrani et al., 1993), as shown in Eqn. 1, where E represents displacement efficiency, as a function of time t, where Q is flow rate, V is the annulus volume, and T_b represents breakthrough time.

$$E(t) = \frac{Qt}{V}, t \le T_b \quad (1)$$

After breakthrough, which is the time of first arrival of the interface at the top of the annulus, the efficiency continues to increase but with a reducing rate due to the amount of cement flowing out of the annulus as it is continued to pump in and leaves by-passed mud in the annulus. The rate of change after breakthrough is an uncertain issue and depends on various parameters as mentioned above. Therefore, in the optimization of cementing job design, maintaining a stable and flat interface between fluids is a key to avoid early breakthrough.

3D CFD Modeling Development and Validation

A Cementing Displacement Experiment

In this section a well-known experimental work conducted by Tehrani et al. (1992, 1993) was introduced. In order to mimic flow conditions similar to actual cases in the cementing of oil wells, the test rig had been specially scaled for experiments. In this experiment setup, Di = 40mm, Do = 50mm, and the total length is 3m, so that the radius ratio for the annulus is comparable to those in the field, i.e. Di/Do = 0.8. The aspect ratio of the annulus (length to width ratio) is around 600. Displacement efficiency was evaluated based on several combinations of variables encountered in the cementing job. Walton and Bittleston (1991) investigated the axial flow of a Bingham plastic in a narrow eccentric annulus. This theoretical solution for steady unidirectional flow had been found to have good agreements with the experiment data with some modification for a yield-power law fluid. The following contents gave some test conditions considered in these experiments:

1) Fluid rheology. Both mud and cement were considered as yield-power law fluids with similar rheologies, or so-called Herschel-Bulkley model: $\tau = \tau_y + K\dot{\gamma}^n$. Typical values of the rheological parameters were: τ_y = 1.22 Pa, K = 0.197 Pa.s^n, and n = 0.505. Fluid displacement with same densities was tested, which was simply considered as single fluid circulation. Positive density difference between cement and mud was also tested to evaluate displacement efficiency. Density differences were $\Delta\rho$ = 0 and $\Delta\rho$ = 16%.
2) Flow rates. In the experiment, various Reynolds numbers were tested to evaluate the impact of flow rates on displacement efficiency. Reynolds numbers ranged from 0.8 to 260. For comparisons, this study borrowed two pairs of Reynolds numbers, Re = 220 and Re = 176, respectively.
3) Eccentricity. Two eccentricity values were tested: e = 0 and e = 0.5.

For non-Newtonian fluids, we use an approach from Antonino Merlo et al. (1995) for the calculation of Reynolds number and is described below. The equivalent Reynolds number in the annulus is required for non-Newtonian fluids instead of Reynolds number, expressed in Eqns. 2-10:

$$Re_{eq} = Ca * Re \quad (2)$$

$$\text{Where } Ca = 1 - \frac{1}{n+1}\left\{\frac{\tau_0}{\tau_0 + k\left[\left(\frac{2(2n+1)}{n(R_2-R_1)}\right)\left(\frac{Q}{\pi(R_2^2-R_1^2)}\right)\right]^n}\right\} \quad (3)$$

$$Re = \frac{2\rho Q}{\mu\pi(R_1+R_2)} \quad (4)$$

$$\mu = \frac{\tau_0 + k\left\{\left[\frac{2(2n+1)}{n(R_2-R_1)}\right]\left[\frac{Q}{\pi Ca(R_2^2-R_1^2)}\right]\right\}^n}{\left[\frac{2(2n+1)}{n(R_2-R_1)}\right]\left[\frac{Q}{\pi Ca(R_2^2-R_1^2)}\right]} \quad (5)$$

$$Q = \pi(R_2^2 - R_1^2)V_a \quad (6)$$

Substituting the above relations in the expression of the equivalent Reynolds number we obtain:

$$Re_{eq} = \left(4\frac{2n+1}{n}\right)\frac{\rho V_a^{(2-n)}(R_2-R_1)^n}{\tau_0\left(\frac{R_2-R_1}{V_a}\right)^n + k\left(2\frac{2n+1}{nCa}\right)^n} \quad (7)$$

While the critical equivalent Reynolds number is given by:

$$Re_{eqcr} = (Ca * Re)_{cr} = \left[\frac{8(2n+1)}{ny}\right]^{\frac{1}{1-z}} \quad (8)$$

Where has been set:

$$y = \frac{log(n)+3.93}{50} \quad (9)$$

$$z = \frac{1.75 - log(n)}{7} \quad (10)$$

If $Re_{eq} < Re_{eqcr}$, the flow is considered laminar while for $Re_{eq} > Re_{eqcr}$, the flow is turbulent flow.

Advanced CFD Simulator

A set of 3-D Computational Fluid Dynamics (CFD) simulations are performed to evaluate displacement efficiency in cementing job, using commercially available CFD software, ANSYS 17.2. For the purpose of validation of the simulation results, Tehrani's 2-phase displacement experiments were used, as explained in the previous section. As we know, in many cases, the flow of fluids in pipe/casing and in annulus is encountered with laminar flow in the cementing job. CFD modeling technique has been used in recent years to unravel the dynamic behavior of fluid movements with reference to cementing (Chen et al., 2014; Xie et al., 2015; Karbasforoushan et al., 2016; Durmaz et al., 2016; Enayatpour and Eric van Oort, 2017).

In this study, we focus on the validation work with Tehrani's experiment data, so all flow conditions should be similar with the experiments, i.e. eccentric annuli, non-Newtonian fluid rheology. Fig. 1 shows a meshed geometry [Elements 119.6 K, Nodes 132 K] for eccentric (e = 0.5) and concentric annuli (e = 0), respectively. Table 1 describes the qualities of grids. Fig. 2 shows a detailed boundary layer near the wall. Failed to define a high resolution in the boundary layer would dramatically alter the flow characteristics. In this content, we only show the cross section of eccentric wellbore because for both concentric and eccentric cases, we can apply the same meshing method.

The VOF (Volume of Fluid) model is a control-volume based, and the most widely used modeling technique to simulate multiphase flows, keeping track of interfaces between different phases. Sharp interfaces between immiscible phases can be captured reliably by using this technique. The volume fraction equation is used to calculate the volume fraction of one (or more) of the phases by solving a continuity equation. For the q[th] phase, the volume fraction equation has the following form (FLUENT Theory Guide 12.0, 2009):

$$\frac{1}{\rho_q}\left[\frac{\partial}{\partial t}\left(\alpha_q\rho_q\right)+\nabla\cdot\left(\alpha_q\rho_q\vec{v}_q\right)=S_{\alpha_q}+\sum_{p=1}^{n}\left(\dot{m}_{pq}-\dot{m}_{qp}\right)\right] \quad (11)$$

where $\dot{m}_{qp}$ and $\dot{m}_{pq}$ are the mass transfer terms. S_{α_q} is the source term. For the primary-phase volume fraction, the following constraint applies in Eqn. 12:

$$\sum_{q=1}^{n}\alpha_q=1 \quad (12)$$

A single momentum equation is solved throughout the whole domain, as shown in **Eqn. 13**, which is dependent on the volume fraction of all phases through the properties ρ and μ:

$$\frac{\partial}{\partial t}(\rho\vec{v})+\nabla\cdot(\rho\vec{v}\vec{v})=-\nabla p+\nabla\cdot[\mu(\nabla\vec{v}+\nabla\vec{v}^{T})]+\rho\vec{g}+\vec{F} \quad (13)$$

In cementing process, the calculation of displacement efficiency is a crucial step for a cementing job design. The interface shape between the two (or more) fluids dictates how effectively the displacement process can be performed. In order to achieve a better displacement and a better bond between casing and wellbore, the interface shape should be as flat and stable as possible. However, in most cases, due to flow path geometry and fluid properties, interface instability such as Rayleigh-Taylor instability (Rayleigh, 1882; Taylor, 1950) could occur if there is a density contrast between fluids. In this study, we also could observe the interface instability in CFD simulations, which is time-dependent.

Validation Results

This developed CFD model was used to compare with Tehrani's experimental results. For validation, mud and cement have similar rheology, modeled as yield power-law model, as mentioned in the study of Tehrani et al. (1993): τ_0 = 1.22 Pa, k = 0.197 Pa.s^n, n = 0.505. A detailed description of simulation cases was shown in Table 2. The developed CFD model was matched with the experimental results up to 1.5 annulus volume pumped fluid, as shown in Fig. 3.

Based on these various cases with available experimental data (Base case, Case 1, Case 2, and Case 3), we can conclude that the CFD model has high reliability with errors as small as 2% to 5% errors in most cases. Displacement efficiency increases linearly with pump rate at the beginning and before the interface of mud and cement firstly arrives the top of the annulus (Breakthrough time). After breakthrough, the displacement efficiency change rate has been largely decreased and causes the displacement efficiency increases gradually, as shown in the results. The inflection point determines the whole displacement efficiency. That also explains why we expect a flat and stable interface between phases. Eccentricity reduces the displacement efficiency compared with concentric annuli. As shown with Base case and Case 1 in Fig. 3, compared with concentric annuli geometry, breakthrough occurs much earlier so that the whole displacement efficiency has been largely reduced in eccentric annuli geometry. By comparing between Case 1 with Reynolds number of 220 and Case 2 of 176, we can observe that pump rate has a slight effect on the displacement. After comparing Case 2 with Case 3, we find a positive density difference can effectively improve displacement efficiency. To our knowledge, the driving force for this type of flow is the hydrostatic pressure imbalance, which could result in azimuthal flow instabilities which accelerate displacement in eccentric annuli, but are likely to leave behind a thin strip of mud in the narrow side, as shown in Fig. 4, generated from CFD modeling. Fig. 5 shows mud concentration profile after 1.56 annulus volume pumping fluid, generated from CFD modeling and our simulator, respectively.

Numerical Simulator

After model validation, this developed CFD model created with ANSYS was compared with our numerical simulator – a mud displacement model. In this study, we conducted numerical simulations using our model (Hu Dai and Gefei Liu, 2017) to calculate displacement efficiency and evaluate the impacts of different factors that affect the results of cement placement process. Simulation studies had proved that pipe/casing rotation was preferred to aid displacement at non-ideal conditions such as high eccentricity wellbores (Enayatpour and Eric van Oort, 2017). For comparisons between these two simulators, we considered the effect of pipe rotation to evaluate the performance of our numerical simulator, with other conditions similar with our previous simulated case (Base case). The cost of simulation time for each case was also pointed out. The details of each simulation case were shown in Table 3.

As we know, the role of pipe rotation had been discussed and displacement efficiency has been well improved with pipe rotation in eccentric cases. The effect of pipe rotation can be observed from Fig. 6, which represent the RPM of 10 (Case 4), 20 (Case 5), 50 (Case 6), and 100 (Case 7), respectively. The comparison results indicate that the discrepancies with these cases were fairly acceptable, especially when the pipe speed was high. A 2D view eccentric unrolled wellbore of mud

displacement generated from our modeling simulator is also given in Fig. 7, showing a variance of mud/cement interface with and without rotation after pumping 3/4 annulus volume. With pipe rotation, the appearance of mud channeling has been largely alleviated and the interface getting more stable and flat.

Moreover, the much shorter simulation time for computation with our numerical simulator made it promising and efficient in cementing design on-site. The comparisons also demonstrated the reliability and robustness of our computer modeling technique for cementing displacement simulation.

Deepwater Intermediate Casing String Simulations

After comparing the simulation performances of our numerical simulator with a validated CFD model, a set of simulations are still needed to deal with deep water intermediate casing string with large diameters. This was done by considering the scenario of cementing a 13 5/8'' intermediate string in 16 ½'' hole, and the total measured depth is 50 ft (15.2 m). Eight scenarios were completed by considering inclination angle, flow rate, and standoff. An overview of the various scenarios with variables was given in Table 4. Scenarios 1-3 tested the effect of inclination angle, and scenarios 1 and 4-6 tested the effect of flow rates. Last, scenarios 1, and 7-8 tested the effect of standoff. Table 5 gave the fluid properties for each scenario.

Mesh Size Sensitivity Analysis

In order to demonstrate the grid independence of the numerical solutions from our simulator, we tested the number of grid sizes used in vertical direction, azimuthal direction, and in radial direction. The first scenario was selected for simulation, and then complete the rest simulations after determined the optimum mesh sizes. Fig. 8 gave the results of simulations after varying the number of grids in three directions. In vertical direction, mesh size of 0.04 m, 0.05 m, and 0.1 m was tested, there was a slight change so we chose 0.1 as the mesh size in vertical direction. In azimuthal direction, we tested the number of 9, 20, 50, and 80 grids, the trend was tended to be stable with increasing number of grids, so the number of 80 was chosen to avoid extremely large computation cost as well as maintaining good simulation results. In radical direction, we tested the number of 15, 20, 30, and 40. The number of 15 was chosen due to a very slight variance of the results.

Simulation Results with Various Scenarios

The importance of casing/drill string rotation for displacement has been understood for decades, and is similar to the beneficial effect of hole cleaning. For all the simulated scenarios listed in Table 4, the drill string was assumed to maintain a rotation speed of 10 RPM. Comparing Scenarios 1-3 as shown in Fig. 9, the deviation angle has little impact on the displacement efficiencies, with an approximated efficiency of 0.83 after pumped one annulus volume of cement. This is attributed to the drill string rotation, where it can almost completely compensate for the negative effects of extreme displacement operations, such as cementing long horizontal casing string in unconventional shale wells. In Fig. 10, we compared the results of efficiencies with the effect of flow rate. In general, displacement efficiency increases with increasing flow rate, as discussed in many studies.

In non-ideal circumstances such as elevated eccentricity, the channeling effect tends to appear in the narrow side of the annulus and forms a channel of by-passed mud. The flow takes place predominantly in the wider annular space. Compared to the concentric annulus of Scenario 1 in Fig. 11, Scenario 7 and Scenario 8 had "early breakthrough" than Scenario 1. After pumped one annulus volume of cement, the concentric annulus had better efficiency and it had the same efficiency with the other two scenarios after pumping 1.7 annulus volumes.

Conclusions

In this study, we use a new 3D CFD model to make comparisons with our modeling technique. The CFD model has been validated with mud-cement displacement experimental works. After making comparisons, we conducted various simulations to investigate displacement in intermediate drill string normally used in deep water well. The effects of inclination angle, flow rate, and standoff were simulated with 8 scenarios. The displacement efficiency at the end of each simulation was captured by integrating the volume of cement fluid contained in the annulus. The simulation results could help the engineers achieve a better understanding of the fluid movements and positions, facilitate to optimize results by identifying optimum parameters mentioned in the above. In general, we can draw some critical conclusions:

1. Our modeling technique generally has good agreement with commercial CFD simulator but with shorter computational time.
2. The simulations emphasize the benefits of pipe rotation in improving cementing efficiency.
3. The present simulator is able to simulate and handle not only eccentric annuli and pipe rotation, fluid rheology, but also real-world scenarios, such as complex well geometries, pump rate adjustments, fluid-fluid intermixing, forward/reverse circulation and wellbore deviations.

Tables

Table 1 Mesh qualities in both concentric and eccentric annuli geometry

NO. Divisions in vertical direction	300
NO. Divisions in azimuthal direction	40
NO. Divisions in radial direction	11
Minimum Orthogonal Quality	5.93E-01
Maximum Ortho Skew	4.07E-01
Maximum Aspect Ratio	5.76E+01

Table 2 List of simulated cases for validation, with flow rates, eccentricity, and fluid densities

Cases	Flow rate	Eccentricity	Pipe rotation	ρ (mud)	ρ (cement)
-	bpm	-	rpm	ppg	ppg
Base case	0.0523	0	0	15.5	15.5
1	0.0523	0.5	0	15.5	15.5
2	0.0456	0.5	0	15.5	15.5
3	0.0417	0.5	0	15.5	17.98

Table 3 List of simulated cases for comparisons between CFD model and our numerical simulator with the effect of pipe rotation

Cases	Flow rate	Eccentricity	Pipe rotation	ρ (mud)	ρ (cement)
-	bpm	-	rpm	ppg	ppg
4	0.0456	0.5	10	15.5	15.5
5	0.0456	0.5	20	15.5	15.5
6	0.0456	0.5	50	15.5	15.5
7	0.0456	0.5	100	15.5	15.5

Table 4. Details of 8 simulated scenarios

Scenario #	Well angle (°)	Flow rate (BPM)	Standoff
1	0	3	100
2	45	3	100
3	90	3	100
4	0	1	100
5	0	5	100
6	0	7	100
7	0	3	70
8	0	3	25

Table 5. Displaced and displacing fluids properties

Fluid 1 (Thin displaced fluid)				
Density (kg/m^3)	K (Pa/s)	n	τ0 (Pa)	Critical shear rate (s^{-1})
1850	0.6	0.54	1.2	10^{-5}
Fluid 2 (Thick displacing fluid)				
Density (kg/m^3)	K (Pa/s)	n	τ0 (Pa)	Critical shear rate (s^{-1})
1800	0.55	0.57	1.5	10^{-5}

Figures

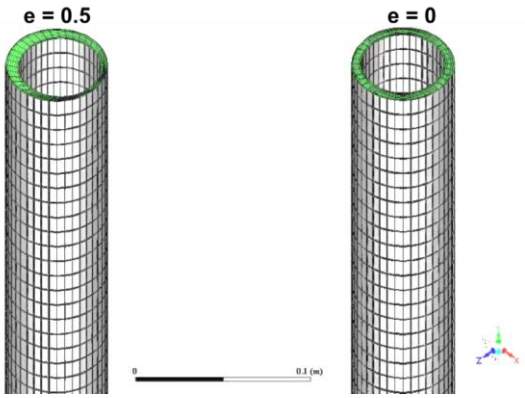

Fig. 1. Meshed annuli geometries of e = 0.5 and e = 0

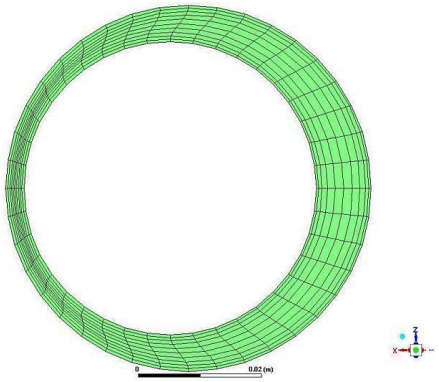

Fig. 2. Boundary layer treatment near the wall (e = 0.5)

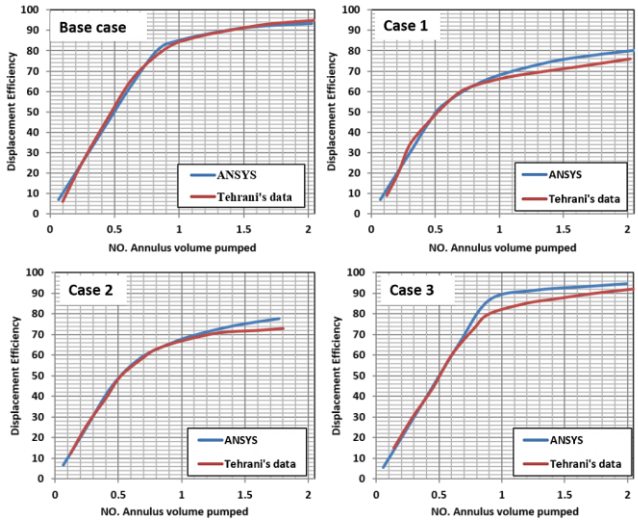

Fig. 3 Validation results with Tehrani's experiment study

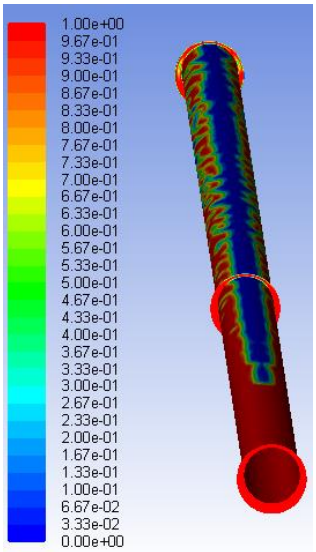

Fig. 4. The volume fraction profile of cement (red) on the casing wall for Case 3 after 1.56 annulus volume pumped, showing mud (blue) lagging behind of the main flow in the narrow side

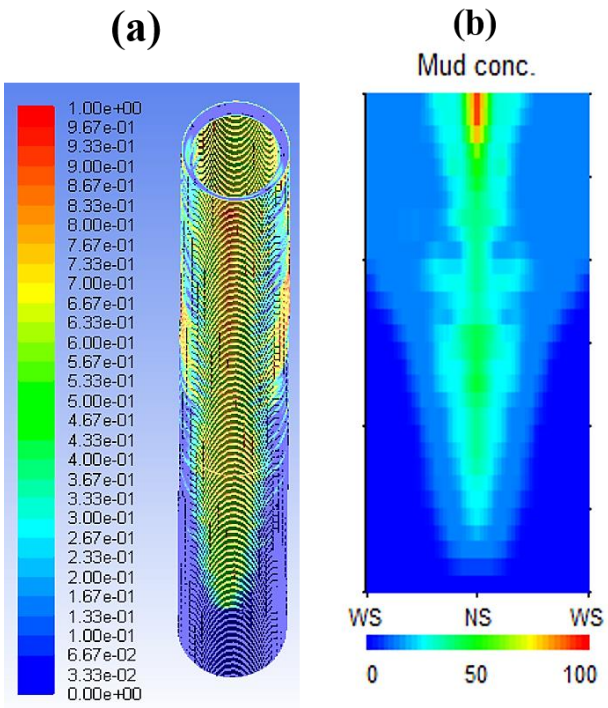

Fig. 5. The mud concentration profile for eccentric annuli with standoff of 50% for Case 3 after 1.56 annulus volume pumped: (a) interior of annulus in CFD model; (b) unrolled interior of annulus in the numerical simulator

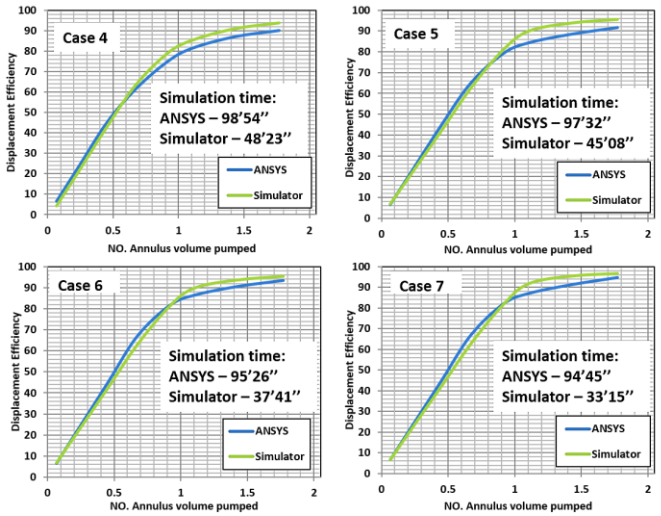

Fig. 6 Simulation Results with the effect of rotation speed on displacement efficiency, a comparison between the CFD model and our simulator

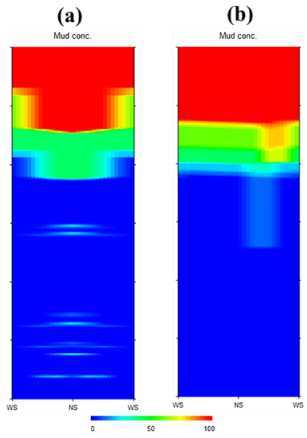

Fig. 7. Mud concentration profiles after 3/4 annulus volume pumped for eccentric annuli with standoff of 50%: (a) without rotation (Case 2); (b) with rotation rate of RPM=50 (Case 6)

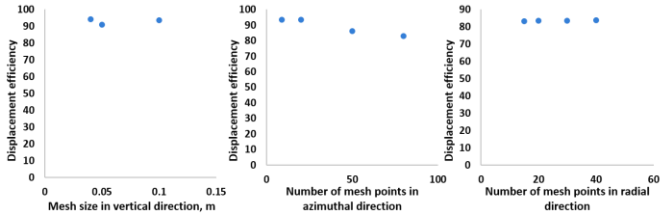

Fig. 8 Selection of optimum grid size for deep water intermediate drilling string simulations

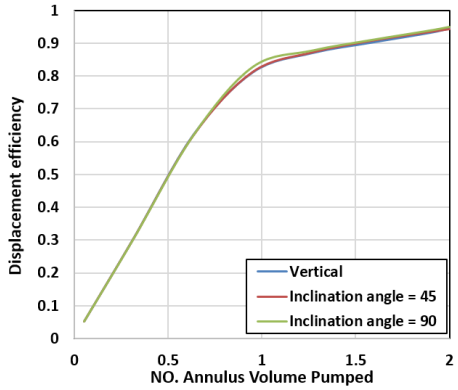

Fig. 9 The effect of inclination angle on displacement efficiency (Scenario 1, 2, 3)

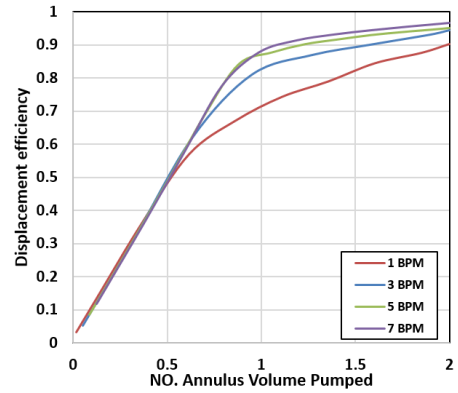

Fig. 10 The effect of flow rate on displacement efficiency (Scenario 1, 4, 5, 6)

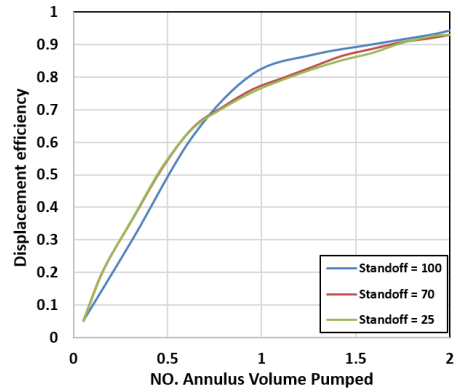

Fig. 11 The effect of standoff on displacement efficiency (Scenario 1, 7, 8)

Acknowledgments

The authors would like to thank Pegasus Vertex, Inc. for technical support and allowing us to present the information in this paper.

Nomenclature

CFD = *Computational Fluid Dynamics*
SO = *Standoff*
VOF = *Volume of Fluid*
RPM = *Revolution Per Minute*

References

1. Antonino Merio, Roberto Maglione, and Cesare Piatti, 1995. An Innovative Model for Drilling Fluid Hydraulics. SPE 29259. Presented at the SPE Asia Pacific Oil & Gas Conference, Kuala Lumpur, Malaysia, 20-22 March 1995.
2. Chen Z., Chaudhary S. and Shine J., 2014. Intermixing of Cementing Fluids: Understanding Mud Displacement and Cement Placement. IADC/SPE 167922. Presented at the 2014 IADC/SPE Drilling Conference and Exhibition, Fort Worth, Texas, 4-6 March.
3. Dai, H. and Liu, G., 2017. Displacement Demystified. Oilfield Technology.
4. Durmaz S., Karbasforoushan H., Ozbayoglu, E.M., Miska, S. Z., Yu M., Takach N., and Aranha P.E., 2016. Mixing of Cement Slurries During Cement Plug Setting. SPE-180338-MS. Presented at the SPE Deepwater Drilling & Completions Conference, Galveston, Texas, 14-15 September.
5. Enayatpour S. and Eric V.O., 2017. Advanced Modeling of Cementing Displacement Complexities. SPE-184702-MS. Presented at the 2017 SPE/IADC Drilling Conference.
6. Farkas, R.F., England, K.W., Roy, M.L., Dickinson, M., Samuel, M. and Hart, Robert E., 1999. New Cementing Technology Cures 40-Year-Old Squeeze Problems. SPE 56537. Presented at the Annual Technical Conference and Exhibition, 3-6 October, Houston, Texas.
7. FLUENT Theory Guide 12.0, 2009. https://www.sharcnet.ca/Software/Ansys/16.2.3/en-us/help/flu_th/flu_th.html (Accessed 4 August 2017).
8. Hemphill T. and Ravi, K., 2006. Pipe Rotation and Hole Cleaning in an Eccentric Annulus. IADC/SPE 99150. Presented at the IADC/SPE Drilling Conference held in Miami, Florida, 21-23 February 2006.
9. Hemphill T. and Ravi, K., 2005. Calculation of Drillpipe Rotation Effects on Fluids in Axial Flow: An Engineering Approach. SPE 97158. Presented at the 2005 SPE Annual Technical Conference and Exhibition held in Dallas, Texas, 9-12 October, 2005.
10. Karbasforoushan H., Ozbayoglu, E.M., Miska, S. Z., Yu M., and Takach N., 2016. On the Instability of Cement-Fluid Interface and Fluid Mixing. SPE-180322-MS. Presented at the SPE Deepwater Drilling & Completions Conference, Galveston, Texas, 14-15 September.
11. Liu, G. and Weber, L., 2012. Centralizer Selection and Placement Optimization. SPE 150345. Presented at the SPE Deepwater Drilling and Completions Conference held in Galveston, Texas, 20-21 June, 2012.
12. Merlo A., Maglione, R., and Piatti, C., 1995. An Innovative Model For Drilling Fluid Hydraulics. SPE 29259. Presented at the SPE Asia Pacific Oil & Gas Conference held in Kuala Lumpur, Malaysia, 20-22 March, 1995.
13. Moroni, N., Ravi, K., Hemphill, T., and Sairam, P., 2009. Pipe Rotation Improves Hole Cleaning and Cement-Slurry Placement: Mathematical Modeling and Field Validation. SPE-124726-MS. Presented at the SPE Offshore Europe Oil & Gas Conference & Exhibition, Aberdeen, UK, 8-11 September 2009.
14. Rayleigh 1882. Investigation of the character of an incompressible heavy fluid of variable density. Proc., London Math. Soc. s1-14 (1): 170-177. doi: 10.1112/plms/s1-14.1.170.
15. Siginer, D.A. and Bakhtiyarov, S.A., 1998. Flow of drilling fluids in eccentric annuli. Journal of Non-Newtonian Fluid Mechanics, Vol 78 pg: 119-132 (1998).
16. Taylor, G.I. 1950. The instability of liquid surfaces when accelerated in a direction perpendicular to their planes. Proc., R.

Soc. London. 201 (1065): 192-196.
17. Tehrani, M.A., Bittleston, S.H., and Long, P.J.G, 1993. Flow instabilities during annular displacement of one non-Newtonian fluid by another. Experiments in Fluids, Vol 14, pg 246-256.
18. Tehrani, M.A., Ferguson, John, and Bittleston, S.H., 1992. Laminar Displacement in Annuli: A Combined Experimental and Theoretical Study. SPE 24569. Presented at the 67th Annual Technical Conference and Exhibition, Washington, DC, 4-7 October.
19. Walton, I.C.; Bittleston, S.H. 1991: The axial flow of a Bingham Plastic in a narrow eccentric annulus. J. Fluid Mech. 222, 39.
20. Xie L., Chaudhary, S., and Chen Z., 2015. Analysis of the Effect of Eccentricity on Displacement of Non-Newtonian Fluid with a Hybrid Method. SPE-174909-MS. Presented at the SPE Annual Technical Conference and Exhibition held in Houston, Texas, 28-30 September, 2015.